Biomass Catalysis

DOI: 10.1002/anie.200((will be filled in by the editorial staff))

A New Route for De-carboxylation of Lactones over Zn/ZSM-5: Elucidation of Structure and Molecular Interactions

*L. Ye[a]†, Q. Song[b]†, B.T.W. Lo[a], J. Zheng[b], D. Kong[b], C.A. Murray[c], C.C. Tang[c] and S.C.E. Tsang[a]**

Abstract: Here, we report the catalytic decarboxylation of gamma-valerolactone, GVL (the biomass derived lactone as an example), over Zn/ZSM-5 to butene, followed by aromatization at high yield with co-feeding of water. The evaluation of catalytic performance at a prolonged time shows that a water molecule is essential to maintain the decarboxylation and aromatization activities without rapid catalyst deactivation. Synchrotron X-ray powder diffraction and Rietveld refinement are then used to elucidate the adsorbed structures of GVL and the immobilized Zn-species with the support of EXAFS and NMR. A new route of cooperative hydrolysis of GVL by the framework Zn-OH and Brønsted acid sites to butene and then to aromatics is *for the first time* demonstrated. The structures and fundamental pathways for the nucleophilic attack of terminal Zn-OH site are comparable to the reported Zn-containing enzymes in biological systems.

Currently, fuels and chemicals are mainly produced from non-renewable oil, coal and gas[1]. However, their depleting supplies, geographically uneven distributions and associated CO_2 emissions are of significant concerns. As a result, identifying an alternative sustainable carbon source for fuel and chemical production is the key role for industry. In fact, biomass has long been regarded as a potential alternative to mitigate these problems. The present low oil prices, as opposed to the high cost of processing biomass, does not yet offer immediate economic incentives. As a result, vigorous research activities are currently sought[2]. Lactones, such as gamma-valerolactone (GVL) can be favourably produced from lignocellulosic biomass[3]. However, only few catalytic studies on the conversions of lactones to useful products have been reported[4,5]. Using the Brønsted acid sites of SiO_2/Al_2O_3, aqueous GVL can undergo ring opening and decarboxylation to form butene. After separation from water, butene gas can be processed into heavier alkenes (for fuels) using amberlyst in a second catalyst bed[5]. Following this work, the direct conversion of GVL to aromatics as platform chemicals via butene without water has also been briefly studied over the Brønsted acid sites in zeolites. However, the low liquid product yield with rapid catalyst deactivation pose technical problems[6]. Furthermore, it would be advantageous to carry out the catalysis without the need for water separation (see SI).

Here, we report that a high yield of aromatic compounds can be produced from a GVL/steam mixture *via* butene at 450 ^oC by feeding an aqueous solution of GVL directly over Zn-modified ZSM-5. The process remains stable for at least 310 hours.

While we realize the interesting potential of this new chemical conversion process, we note that the Zn incorporation into H-ZSM-5 gives much superior catalytic activity than the pure H-ZSM-5. One would be interested to find out how the Zn/ZSM-5 structure provides for such efficient conversion. It is interesting to note that nature also selects the element Zn to catalyze acid-base hydrolysis reactions in cellular and extra-cellular environments. This is because of its higher effective nuclear charge (Z_{eff}) among the transition metals, rapid water-exchange and no complications from the redox properties. For example, carbonic anhydrase (CA) enzymes containing Zn^{2+} [7] are used to catalyze the reversible hydration of CO_2. Similarly, Zn^{2+} containing beta-lactamase (BL) enzymes[8] can rapidly hydrolyze the lactam groups in penicillins. With the specific Zn structure in these enzymes, their turnover frequency can reach 10^6-10^7 s^{-1} (the diffusion rate limit of water), making them the most 'active' and kinetically 'perfect' of all enzymes[9].

Due to the intrinsic shape and size selectivity as well as single-site confinement, zeolite catalysts have long been regarded as 'solid enzymes'[10]. In addition, two or more catalytically active sites may work in a cooperative manner, giving unusual properties[11]. The introduction of Lewis metal ion sites into zeolites containing excess Brønsted acid sites may create a synergistic effect in catalysis. In the present case, GVL contains a reactive lactone group with a carbonyl that could be susceptible to ring opening as the first step in hydrolysis by these sites. In order to understand this new conversion, the information on the structure of the active Zn sites with respect to the Brønsted acid sites and their interactions with the GVL in the Zn/ZSM-5 is crucial.

Recently, the significant advancement of modern diffraction facilities using high brightness synchrotron has provided chemists with a powerful tool in studying porous but crystalline materials. For example, high resolution synchrotron X-ray powder diffraction (SXRD) data was used to determine the structure of various zeolites[12,13]. We have also recently reported the use of SXRD combined with Rietveld refinement to elucidate organic adsorbate structures in zeolites. The alteration in scattering parameters of the modified framework atoms by the molecules enables the probing of adsorption geometries and interactions with the Brønsted acid sites in terms of atomic distances and angles[14,15]. Thus, the environment of Zn and the adsorption geometry of GVL were elucidated by SXRD in combination with EXAFS and ^1H MAS NMR. The obtained structures are compared to that of 'perfect' CA II enzyme with a view of rationalizing this unique catalysis and providing hints for further improvement.

The Brønsted acidic sites in H-ZSM-5 may further catalyze butene to aromatic compounds[6,16]. Thus, some pure and metal-modified ZSM-5 catalysts were tested using a flow reactor in SINOPEC (SRIFT) by feeding a continuous liquid flow of 40 wt% GVL/H_2O with weight hourly space velocity (WHSV) of 1.0 h^{-1} to a catalyst zone at 450 ^oC (with a preheated zone) under industrial applicable conditions. As seen in Figure 1a, the catalytic performances of some ZSM-5 based catalysts are compared (SI Section 2). The GVL conversions are generally found to be greater than 99% (complete conversion) within 12 hours of reaction time for all the catalysts studied (Figure S1b). For the unmodified H-ZSM-5 sample, the total aromatics (benzene, toluene, xylene (BTX) and higher alkyl aromatics) selectivity is about 62% with the light alkane/alkene selectivity reaching 38%. As stated, GVL can undergo ring opening and decarboxylation to form the initial butene[5,6], but H-ZSM-5 alone appears to be insufficient to generate aromatics at

[a] Dr Lin Ye[†], Benedict T.W. Lo, Prof S.C. Edman Tsang*
Department of Chemistry, University of Oxford, Oxford, OX1 3QR (UK),
E-mail: edman.tsang@chem.ox.ac.uk;

[b] Dr Qi Song[†], Dr Junlin Zheng and Prof Dejing Kong
Shanghai Research Institute of Petrochemical Technology SRIPT-SINOPEC, Shanghai 201208 (China); [†] co-first authorship

[c] Dr Claire A. Murray, Prof Chiu C. Tang
Diamond Light Source Ltd, Harwell Science and Innovation Campus, Didcot, Oxfordshire, OX11 0DE (UK)

[*] The authors wish to thank EPSRC, UK and Diamond Light Source Ltd and SRIFT-SINOPEC for the financial support of this collaborative work and are grateful to the Office of China Postdoctoral Council to grant a fellowship to LY to work at Oxford.

Supporting information is given via a link at the end of the document.

high selectivity. The addition of particularly Sn, Ga and Zn can significantly increase the aromatics selectivity at the expense of light alkane/alkene, presumably due to the introduction of other active sites through these metal ions doping. Among the screened samples, Zn/ZSM-5 gives the highest aromatics selectivity of 91.4% which is about 30% higher than the unmodified H-ZSM-5. The carbon balance was found to be 99 ± 1%, while coke and gaseous products accounted for 2.4% and 7.2% of the total carbon detected, respectively. The major gas phase product was found to be 1-butene (4.8%, see SI Section 2).

Figure 1b shows the long-term evaluation of the catalytic performance of the Zn/ZSM-5 catalyst. There is a small but progressive decrease of GVL conversion over 310 h due to 'carbon' deposition but with a marginal change in total aromatics selectivity. It is interesting to note that feeding the same amount of GVL in nitrogen without water gives a much lower aromatic yield (*ca.* 50%). It also shows an extremely fast deactivation, indicating the important role of *water* in this catalyzed decarboxylation/aromatization reaction. Since this effect was not yet reported in previous studies[6], further investigation is hereby conducted. The evaluation of the Zn/ZSM-5 catalyst under repeated, accelerated deactivation and re-activation steps (switching nitrogen carrier to air and calcining the sample at 600 ^{o}C for 1 h) shows that the activity of the Zn/ZSM-5 is totally regained (Figure S2). The high catalytic activity, good lifetime and recyclability of Zn/ZSM-5 make it a promising candidate for the decarboxylation reaction of lactones (GVL) in water in future bio-processing. Perhaps, there are a number of key questions that remain to be answered: why does Zn^{2+} modification give the best activity for the formation of aromatics via butene from GVL/H_2O over the tested catalysts? How does the active site interact with GVL? Why does H_2O appear to be essential for the catalysis? How do the structure and catalytic mechanism of the decarboxylation reaction by this Zn-containing zeolite differ from those of Zn enzymes in nature? It is noted that structure of enzymatic catalyst and pathway can be elucidated through the growth of corresponding single crystal enzyme structure and substrate-enzyme complex. However, it would not be applicable to industrial powder zeolite based catalysts even if they are regarded as 'solid enzymes'. On the other hand, the structure of Zn/ZSM-5 and the substrate-active site interaction in the zeolite, if known, could provide important hints to the catalytic activity. As a result, SXRD combined with Rietveld refinement was used, for the first time, to monitor the coordination environment of the Zn species in the zeolite. The Zn environment reflects the nature of the interaction between Zn, the GVL molecule and water during the first step in aromatization over the Zn/ZSM-5 catalyst. All the data were refined by the Rietveld method using TOPAS Academic refinement software (Bruker AXS, version 5), see analytical details in SI Section 3.

First, by comparing the SXRD patterns of fresh unmodified H-ZSM-5 with and without Zn incorporation, the relative intensity of the peaks changed between the two samples without peak broadening or formation of other ZnO crystalline peaks (Figure S3). As mentioned in the method section, more than 4,000 independent *hkl* reflections have been used for the refinement calculations, which allow a greater number of structural variables to be refined in satisfactory manner. The quality of the Rietveld refinements of SXRD data was confirmed with low R-weighted pattern (R_{wp}) values and goodness-of-fit factor (Tables S1-S5). The structural details and Brønsted acid site (at the framework T6 site) information of our H-ZSM-5 have been characterized in our previous work[14,15].

Figure 2a (also Figure S6) and the refinement result clearly show the space group of the fresh and regenerated Zn/ZSM-5 from 310 h by air treatment remains as *Pnma* as in a typical H-ZSM-5. Two isolated Zn species with electron rich regions have been identified within the zeolite cavity. One Zn^{2+} (named Zn-1) is found located at the intersection region of the sinusoidal and straight channels.

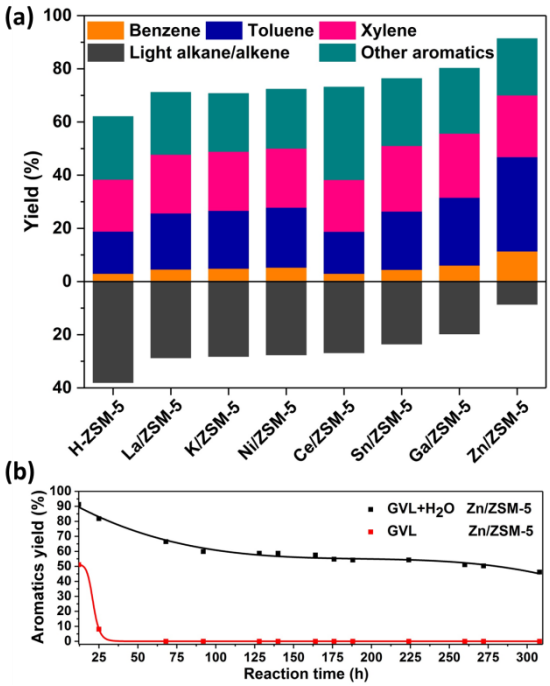

Figure 1. (a) Product distribution over various ZSM-5 based catalysts (5 g) by feeding 40 wt% aqueous GVL solution to the preheated catalyst bed with WHSV 1.0 h^{-1} at 10 bar after 12 h (the time to collect the liquid products for analysis) at complete GVL conversions. The mole % yield is based on mol. GVL to products (see SI Section 1). (b) Long term catalytic performance of Zn/ZSM-5 with WHSV 1.0 h^{-1} at 450 ^{o}C.

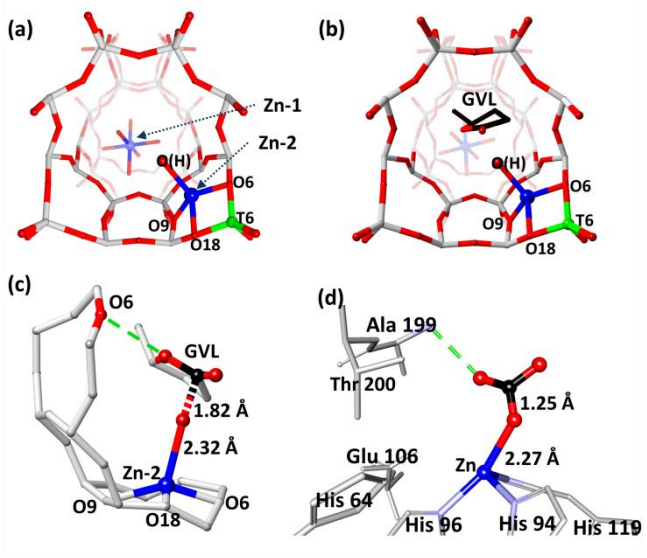

Figure 2. The refined structures of Zn/ZSM-5 catalyst derived from SXRD and refinements. (a) Fresh (Figure S4) and regenerated Zn/ZSM-5 (Figure S6); (b) GVL adsorbed on fresh Zn/ZSM-5 (Figure S5); (c) A close-up view of Zn(2)-OH interacting with the carbonyl of GVL; (d) A published crystal structure showing a complex intermediate of Zn-OH of T199A-CA II enzyme with adsorbed CO_2 for comparison (PDB: 1CAM) [Crystal Database from National Center for Biotechnology Information][19]. In all the refined structures, the stick/ball model is used O = red, Si = grey, Al = green, Zn = blue, C = black. In (c) and (d), only the activated complexes with carbonyl adsorbates are colored. A mirror plane symmetry has been disregarded for clarity, view down the x-axis (the sinusoidal channel).

By including a hexa-aqua Zn-1 species into the Rietveld refinement, a good fit with the experimental data has been clearly achieved. This entrapped Zn-1 with the 6 equivalent non-framework O as a typical hexa-aqua Zn^{2+} gives an average Zn-$O(H)_2$ distance of 2.12(3) Å (Table S6 and SI). Its location in the porous cavity of Zn/ZSM-5 is likely maintained by the surrounding negatively charged framework oxygens through electrostatic interaction by ion-exchange with the Brønsted acid

sites. The site occupancy factor (SOF) of the Zn-1 is 0.104(2). Taking the symmetry of the *Pnma* space group into account, there are 0.104 × 4 = 0.42 Zn-1 per unit cell of Zn/ZSM-5. Interestingly, a *tetrahedrally coordinated* Zn (named Zn-2) attached to the 5-membered ring of ZSM-5 through the wall-oxygens next to Al(T6) is also identified. The SOF of Zn-2 is 0.071(3) corresponding to 0.071 × 8 = 0.57 Zn-2 per unit cell. Thus, a total of 0.99 Zn per unit cell is obtained, which is in agreement with the value derived from ICP-MS of 0.97 Zn per unit cell. The k^3-weighted Fourier transformed EXAFS data of the fresh Zn/ZSM-5 were measured at the Zn K-edge, using ZnO as a standard (Table 1 and Figure S7). A k^1-k^2-k^3 fitting procedure in K- and R-space was carried out to identify the presence of any Zn-O or Zn-Zn interactions in the first shell and Zn-O in the second shell. The fitting result shows an averaged bond length and coordination number (CN) of the Zn/ZSM-5. It is clear that the average bond length of 2.07(1) Å is related to the backscattering from the oxygen atoms to the directly bonded Zn. There is no evidence for the possible Zn-Zn nearest bond distance of 2.3 Å or second shell Zn-O bond distance of 3.0 Å of the ZnO lattice in the Zn/ZSM-5 EXAFS spectrum. This result undoubtedly indicates that the Zn species in Zn/ZSM-5 are isolated without any ZnO aggregates or clusters, which is consistent with the SXRD result. The average CN of 5.2(2) from the EXAFS fitting matches the calculated average CN of 4.8(2) derived from 57% four coordinated Zn (Zn-2) and 42% six coordination Zn (Zn-1), according to the SOFs of the SXRD refinement. Also, the derived Zn-O distance of 2.07(1) or 2.06(1) Å from EXAFS data is close to the averaged bond distance of 2.11(2) Å of the two Zn species from the SXRD data (Tables S2-S6).

According to the refined structure of the tetrahedral Zn-2 site surrounded by four oxygens (Figure 2a), it is clear that this Zn^{2+} is directly immobilized with the framework oxygens: O6, O18 and O9 sites following the ion-exchange and subsequent calcination of Zn/ZSM-5. The derived bond distances of Zn-2-O6, Zn-2-O18 and Zn-2-O9 correspond to 1.92(2), 1.95(2) and 2.19(3) Å, respectively from the SXRD and refinement. Although H atoms cannot be located by SXRD due to their low electron density, the remaining non-framework oxygen of 2.32(5) Å with Zn is identified in the form of Zn-2-O(H) as demonstrated by our ^{1}H-NMR and Raman spectroscopy, as shown later. Thus, this hydrated Zn^{2+} after ion-exchange and calcination likely loses some of its coordinated water. It is then immobilized onto the framework oxygens which contain one of the acid sites. The formation of the terminal Zn-OH initially looks puzzling, as Zn^{2+} itself cannot activate water molecule at moderate temperature.

Table 1. Comparison between the refined structural models from SXRD and best-fit EXAFS data.

Zn/ZSM-5 Catalyst		CN^{SXRD}	CN^{EXAFS}	R^{SXRD} (Å)	R^{EXAFS} (Å)	Debye-Waller (Å)	E_{not} (eV)
Fresh	**Zn-O**	**4.8(2)**	**5.2(2)**	**2.11(2)**	**2.07(1)**	**0.007(1)**	**3.4**
Regenerated	**Zn-O**	**5.0(2)**	**5.0(1)**	**2.11(2)**	**2.06(1)**	**0.009(1)**	**4.6**

Statistical errors are displayed in brackets; CN stands for coordination number; R represents derived atomic distance (see SI Section 4).

Nevertheless, the strong nucleophilic nature of terminal Zn-OH [5a] (i.e. the new active site) if formed can attack the carbonyl group of GVL. Through ring opening, CO_2, butene and water are produced via Zn-OH nucleophilic attack This offers an alternative to the simple acid hydrolysis route by the Brønsted acid sites (framework or extra-framework) that equally forms butene and CO_2 as a result [5b]. We observe higher rate and selectivity for GVL conversion to aromatics via butene over Zn/ZSM-5 than H-ZSM-5 as shown in Figure 1. It clearly suggests that Zn-OH is more active and selective for such conversion. However, we cannot exclude the possibility of GVL that may also interact with Zn-1 (presumably via one of its coordinated saturated H_2O ligand) and contribute to the overall catalytic activity. It is because our approach cannot apply to those GVL-Zn-1 species if they are non-crystallised and hence cannot rule out their existence. Despite the polarisation by Zn^{2+} it is however envisaged that the non-dissociated H_2O molecule cannot act as a strong nucleophile as that of Zn^{2+}-OH^- for the rapid GVL attack. Similarly, without the presence of Zn^{2+}, the BAS sites are also unable to polarize a water molecule to asymmetric OH^- and H^+. The key question is how this Zn-OH site can be regenerated during the catalysis with water co-feeding. It should be noted that the terminal Zn-OH is located adjacent to the original Brønsted acid site in other asymmetrical units (T6). Previous DFT calculations indicated one of the coordinated water molecules on divalent metal cations such as Zn^{2+} can dissociate when they are introduced into the framework of H-ZSM-5 via ion-exchange[17,18]. This water dissociation is energetically favored, resulting in the formation of a hydroxyl group bonded to the metal cation and the regenerated proton residing on a nearby ionized Brønsted acid site (see SI for further information). Thus, the cooperative dissociative activation of water molecule that regenerates Zn-OH with a deprotonated Brønsted acid site to complete the catalytic cycle is plausible, based on our structural findings. Figure 2b depicts the crystal structure of adsorbed GVL on Zn/ZSM-5 by SXRD and Rietveld refinement. Despite there are the two Zn species (i.e. Zn-1 and Zn-2) in our Zn/ZSM-5, the carbonyl of GVL molecule only aligns itself to the terminal hydroxyl group of Zn-2. A closer inspection of the adsorption geometry (Figure 2c) suggests the formation of a strong dative bonding between the GVL and Zn-OH with a short O-$C_{carbonyl}$ distance of 1.82(4) Å. In contrast, no interaction of GVL with the Zn-1 species in the structure is found. We also note that the Zn-OH at the Zn-2 site in Zn/ZSM-5 is structurally comparable to the active site of the CA II enzyme (Figure S4d 1CA2). The active Zn^{2+} site is similarly tetrahedrally coordinated, but with three histidine groups and a terminal -O(H)[19]. During bio-catalysis, the -OH of the amino acid in site 199 near the Zn^{2+} is known to activate the incoming water molecules. Hence, terminal Zn-O(H) and H^+ through hydrogen bonding interaction are formed. They have an analogous proton accepting role like our ionized T6 site in a similar atomic spatial position in Zn/ZSM-5 as previously discussed. The nucleophilic OH^- can then attack CO_2 to form a Zn-hydrogen carbonate species. Thus, this enzymatic Zn^{2+} catalyzes the conversion of CO_2 and H_2O to HCO_3^- and H^+ with extremely high TOF[20]. Figure 2d shows the published crystal structure of the T199A CAII enzyme-CO_2 complex from the crystal database of the National Center for Biotechnology Information[19]. Interestingly, the adsorption geometry of GVL in the zeolite by the terminal Zn-OH as shown in Figure 2c and the configuration of the Zn-containing enzyme-CO_2 complex are alike. Scheme S2 (SI Section 8) demonstrates the proposed mechanism for butene production by the cooperative ring opening and hydrolytic decarboxylation of gamma-valerolactone (GVL) and water activation over Zn/ZSM-5, followed by regenerating Zn-OH and Brønsted acid site. As seen in the proposed mechanism (SI Sections S8-10), a water molecule directly participates in the hydrolysis mechanism for the decarboxylation of GVL, in a similar manner to that seen in the 'perfect' Zn-enzymes. This mechanism is consistent with our labelled experiment showing the formation of $C^{16/18}O_2$ when $H_2{}^{18}O$ was used (SI Section 5). Thus, water is not only required to reduce 'carbon' deposition, but also acts as a catalyst to produce CO_2 and butene from GVL over the Zn-OH and Brønsted acid site in a cooperative manner. The butene, once formed, is known to undergo aromatization over H-ZSM-5 based materials to give aromatics; this has been well studied and will not be further discussed here[21].

As mentioned, the Zn/ZSM-5 catalyst is a typical microporous acidic zeolite. It exhibits a slow but progressive deactivation during 310 h of on-stream testing. However, the deactivated Zn/ZSM-5 catalyst can be fully regenerated through air calcination at 600 ^oC for 1 h. The same concentration of Zn (0.99 Zn per unit cell) is obtained, by summing the SOFs of Zn-1 and Zn-2 (Table S5). Similarly, the derived coordination numbers and corresponding Zn-O distances from SXRD refinement and

EXAFS (Table 1 and Table S6) of the regenerated sample also clearly indicate the structural integrity of the active site in Zn/ZSM-5 after the prolonged testing (see SI Sections 6, 7 and Figure S9). The structure and ability for nucleophilic attack of Zn/ZSM-5 and Zn-containing enzymes resemble to each other. Thus, this suggests that the immobilized tetravalent Zn^{2+} with the terminal -OH is the common active site.

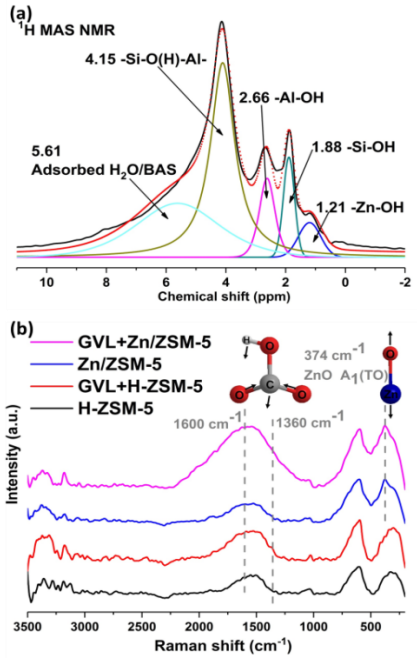

Figure 3. (a). ^{1}H MAS NMR of fresh Zn/ZSM-5 at 30 ^{o}C, after vacuum pre-treatment at 300 ^{o}C for 8 h, experimental data (black line), simulated data (red dot) and the corresponding simulated partial contributions (blue, green, violet, dark yellow and light blue line). (b) Raman spectra of various samples. They show clearly a characteristic large peak and wide broadening of Raman absorption frequencies near 1100-2240 cm^{-1} which encompasses -C=O of GVL at *ca.* 1600 cm^{-1} and symmetrical O-C-O at 1360 cm^{-1} upon the GVL adsorption on Zn/ZSM-5. In addition, the A_1 (TO) mode of Zn-O at 374 cm^{-1} is visible on the terminal Zn-OH in Zn/ZSM-5.

However, they should not be taken for a direct like-for-like comparison in mechanism. The initial step of nucleophilic attack of GVL by Zn-OH during hydrolysis requires a bond cleavage with a higher activation barrier than that of the dehydration/hydration of the more labile CO_2 in the enzymatic reaction without bond breakage. In addition, the Zn^{2+} is immobilized by the 'O' ligands (Si-O-Si) of the rigid zeolite framework. It is hence electronically and structurally different from those of the flexible prosthetic hydrophobic protein chain in the case of Zn-containing enzymes. We understand that even if this heterogeneous catalyst contains sites that are geometrically akin to enzymes, the reaction temperature, conditions, interactions with the framework, adsorption and desorption processes still make this system significantly different. Nevertheless, the tetrahedral structure of Zn-2 with a terminal nucleophilic Zn-OH for the hydrolysis and its regeneration by a neighbouring H^+ acceptor site, which activate a water molecule in a cooperative manner, is clearly comparable in both cases. It is also noted that the nucleophilicity of M-OH over our tested catalysts also follows the order of Zn > Ga > Sn. This trend can be rationalised by the order of electronegativity: Zn(1.65) < Ga(1.81) < Sn(1.96). Hence, the electron density of the 'O' of the M-OH group follows the trend: Zn-OH > Ga-OH > Sn-OH.[5a] Since the regenerative formation of nucleophilic Zn-OH by GVL and water in this enzyme-mimic Zn/ZSM-5 is an important key feature, it is crucial to experimentally verify the existence of the Zn-OH active site. Figure 3a shows five resolved ^{1}H MAS NMR signals of the fresh Zn/ZSM-5 at 1.21, 1.88, 2.66, 4.15 and 5.61 ppm assigned to Zn-OH, Si-OH, Al-OH, H^+ of Brønsted acid site and the H of adsorbed H_2O on Brønsted acid site, respectively. The latter four signals have been previously detected in various aluminosilicate-based zeolites[22] but the former peak is reflected by the characteristic Zn-OH in Zn/ZSM-5[23].

Raman spectroscopy was also employed to study the adsorbed structure of GVL on Zn/ZSM-5. Figure 3b shows a much larger and broader peak with Raman frequencies at the 1100-2240 cm^{-1} region which encompasses -C=O of GVL at *ca.* 1600 cm^{-1} and symmetrical O-C-O at 1360 cm^{-1} [24] upon GVL adsorption on Zn/ZSM-5. In addition, the A_1(TO) mode of Zn-O at 374 cm^{-1} [25] is clearly visible upon the adsorption of GVL on the terminal Zn-OH in Zn/ZSM-5.

In conclusion, using SXRD combined with Rietveld refinement, we demonstrate for the first time an anchored Zn-OH structure in Zn/ZSM-5 can adsorb GVL via a strong Lewis acid-base interaction. The regenerative Zn-OH and a neighbour Brønsted acid site in H-ZSM-5 by dissociative adsorption of water molecule work in a cooperative manner. They provide new catalytically active sites for a cascade of reactions to form aromatics via butene. The structure and mechanism for the nucleophilic attack of the active Zn-OH site appears are comparable to that of the reported CA II enzyme. Hence, it can be regarded as an efficient 'solid enzyme' for this reaction. Thus, the immobilized Zn^{2+} for catalytic hydrolysis may provide inspirations to the chemical industry on how to harness biomass to produce useful products.

Keywords: Zn/ZSM-5 • gamma-valerolactone • decarboxylation • synchrotron X-ray powder diffraction • Rietveld refinement

[1] M. R. Rahimpour, M. Jafari, D. Iranshahi, Appl. Energ. **2013**, 109, 79-93.
[2] W. R. H. Wright, R. Palkovits, Chemsuschem **2012**, 5, 1657-1667.
[3] D. M. Alonso, S. G. Wettstein, J. A. Dumesic, Green Chem. **2013**, 15, 584-595.
[4] I. T. Horvath, H. Mehdi, V. Fabos, L. Boda, L. T. Mika, Green Chem. **2008**, 10, 238-242.
[5] (a) A. L. Allred, J. Inorg. Nucl. Chem. **1961**, 17, 215-221.
(b) J. Q. Bond, D. M. Alonso, D. Wang, R. M. West, J. A. Dumesic, Science **2010**, 327, 1110-1114.
[6] H. Xia, J. Zhang, X. Yan, S. Xu, L. Yang, J. Fuel. Chem. Technol. **2015**, 43, 575-580.
[7] in Carbonic Anhydrase: Mechanism, Regulation, Links to Disease, and Industrial Applications, Vol. 75 (Eds.: S. C. Frost, R. McKenna, S. C. Frost, R. McKenna), **2014**.
[8] J. Brem, S. S. van Berkel, W. Aik, A. M. Rydzik, M. B. Avison, I. Pettinati, K.-D. Umland, A. Kawamura, J. Spencer, T. D. W. Claridge, M. A. McDonough, C. J. Schofield, Nature Chem. **2014**, 6, 1084-1090.
[9] D. N. Silverman, S. Lindskog, Acc. Chem. Res. **1988**, 21, 30-36.
[10] D. H. Olson, G. T. Kokotailo, S. L. Lawton, W. M. Meier, J. Phys. Chem. **1981**, 85, 2238-2243.
[11] C. P. Grey, F. I. Poshni, A. F. Gualtieri, P. Norby, J. C. Hanson, D. R. Corbin, J. Am. Chem. Soc. **1997**, 119, 1981-1989.
[12] R. E. Morris, S. J. Weigel, N. J. Henson, L. M. Bull, M. T. Janicke, B. F. Chmelka, A. K. Cheetham, J. Am. Chem. Soc. **1994**, 116, 11849-11855.
[13] P. Norby, J. Am. Chem. Soc. **1997**, 119, 5215-5221.
[14] B. T. W. Lo, L. Ye, J. Qu, J. Sun, J. Zheng, D. Kong, C. A. Murray, C. C. Tang, S. C. E. Tsang, Angew. Chem. Int. Ed. **2016**, 55, 1-5.
[15] L. Ye, B. T. W. Lo, J. Qu, I. Wilkinson, T. Hughes, C. A. Murray, C. C. Tang, S. C. E. Tsang, Chem. Commun. **2016**, 52, 3422-3425.
[16] H. Kitagawa, Y. Sendoda, Y. Ono, J. Catal. **1986**, 101, 12-18.
[17] G. Yang, Y. Wang, D. H. Zhou, X. C. Liu, X. W. Han, X. H. Bao, J. Mol. Catal. A: Chem. **2005**, 237, 36-44.
[18] A. N. Subbotin, G. M. Zhidomirov, I. R. Subbotina, V. B. Kazansky, Kinet. Catal. **2013**, 54, 744-748.
[19] Y. F. Xue, A. Liljas, B. H. Jonsson, S. Lindskog, Proteins: Struct., Funct., Genet. **1993**, 17, 93-106.
[20] Z. Fisher, J. A. H. Prada, C. Tu, D. Duda, C. Yoshioka, H. Q. An, L. Govindasamy, D. N. Silverman, R. McKenna, Biochemistry **2005**, 44, 1097-1105.
[21] Y. Ono, H. Kitagawa, Y. Sendoda, J. Chem. Soc., Faraday Trans. **1987**, 83, 2913-2923.
[22] L. Heeribout, C. Doremieux-Morin, J. P. Nogier, R. Vincent, J. Fraissard, Microporous Mesoporous Mater. **1998**, 24, 101-112.
[23] J. F. Wu, S. M. Yu, W. D. Wang, Y. X. Fan, S. Bai, C. W. Zhang, Q. Gao, J. Huang, W. Wang, J. Am. Chem. Soc. **2013**, 135, 13567-13573.
[24] E. Garand, T. Wende, D. J. Goebbert, R. Bergmann, G. Meijer, D. M. Neumark, K. R. Asmis, J. Am. Chem. Soc. **2010**, 132, 849-856.
[25] Y. Dong, C. Feng, P. Jiang, G. Wang, K. Li, H. Miao, Rsc Adv. **2014**, 4, 7340-7346.

Entry for the Table of Contents (Please choose one layout)

Layout 1:

COMMUNICATION

A new cooperative ring-opening route for decarboxylation of gamma-valerolactone (biomass derivative lactone) with water molecule activation over Zn/ZSM-5 catalyst by the regenerative Zn-OH and Brønsted acid site to CO_2 and 1-butene. The structures and fundamental pathways are comparable to that of reported Zn-containing enzymes in biological systems.

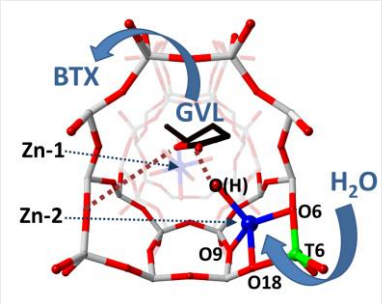

*Lin Ye, Qi Song, Benedict T.W. Lo, Junlin Zheng, Dejing Kong, Claire A. Murray, Chiu C. Tang, Shik Chi Edman Tsang**

Page No. – Page No.

A New Route for De-carboxylation of Lactones over Zn/ZSM-5: Elucidation of Structure and Molecular Interactions